

Mode identification for Balloon 090100001 using combined multicolour photometry and spectroscopy

A. Baran^{1,2*}, A. Pigulski³, S.J. O’Toole⁴

¹*Cracow Pedagogical University, ul. Podchorążych 2, 30–084 Kraków, Poland*

²*Toruń Centre for Astronomy, ul. Gagarina 11, Toruń, Poland*

³*Instytut Astronomiczny Uniwersytetu Wrocławskiego, ul. Kopernika 11, 51–622 Wrocław, Poland*

⁴*Anglo-Australian Observatory, PO Box 296, Epping 1710, Australia*

Accepted . Received ; in original form

ABSTRACT

In this paper, we show that method of mode identification using combined multicolour photometry and spectroscopy can be successfully applied to the pulsating subdwarf B star Balloon 090100001. The method constrains the spherical degree, ℓ . We confirm that the dominant mode is radial and we show that for some other modes the method provides values of ℓ consistent with the observed rotationally split triplet. Moreover, we derive a radius variation of 1.7 per cent for the dominant mode. The identification opens the possibility for constraining the internal structure of the star by means of seismic methods.

Key words: oscillations – subdwarf – stars: individual: Balloon 090100001.

1 INTRODUCTION

About a decade ago, pulsations in hot subdwarfs (sdB) were discovered by astronomers at the South African Astronomical Observatory (Kilkenny et al. 1997, and subsequent papers in the series). At present, there are two classes of pulsating hot subdwarfs (sd-BVs) known: V361 Hya and PG 1716 stars. The former pulsate in p modes which have short periods, typically a few minutes long, the latter, in g modes which have periods an order of magnitude longer. Some V361 Hya stars show relatively large amplitudes, reaching or even exceeding 50 mmag in V , while for PG 1716 stars only low-amplitude modes are observed. The two classes also have slightly different effective temperatures, V361 Hya stars are on average hotter than PG 1716 stars.

Considering the poorly understood evolutionary history of sdB stars, it is very important to obtain information on their internal structure whenever possible. The discovery of pulsations in sdB stars has opened a new avenue to probe their interiors by means of seismic techniques. However, a prerequisite of a successful application of asteroseismology is detection of at least several modes which are properly identified in terms of their pulsation geometry. The identification can be carried out using different methods that utilize photometric or spectroscopic data or a combination of both.

For sdBV stars, spectroscopic methods have an extra layer of difficulty because the currently known objects are fainter than $V \approx 12$ mag, and they all have very short pulsation periods. Good time-resolved spectroscopic observations can therefore only be obtained using large telescopes. For this reason, there have been many attempts to use only (multicolour) photometric data to

identify modes in sdBV stars. In particular, methods that compare observed and theoretical behaviours of pulsation amplitude with wavelength have been used to constrain the spherical degree, ℓ . For example, such applications have been presented by Koen (1998) for KPD 2109+4401, Jeffery et al. (2004) for HS 0039+4302 and Jeffery et al. (2005) for PG 0014+067. Unfortunately, photometric data are limited because the amplitude ratios of modes with different ℓ sometimes have very similar wavelength dependence (see Ramachandran, Jeffery & Townsend 2004), and therefore this does not lead to an adequate discrimination of ℓ . In the best case, only some possibilities could be rejected (see Sect. 5 or Tremblay et al. 2006).

Despite the difficulties in obtaining good-quality, time-resolved spectra for sdBV stars, spectroscopic time-series data have been obtained for some of the brightest objects: for example, PG 1605+072 = V 338 Ser (O’Toole et al. 2000, 2002, 2003, 2005; Woolf, Jeffery & Pollacco 2002; Falter et al. 2003), KPD 2109+4401 and PB 8783 (Jeffery & Pollacco 2000), PG 1627+017 (For et al. 2006) or Balloon 090100001 (hereafter Bal09; Telting & Østensen 2006, hereafter TO06). In this paper we show that the method of Daszyńska-Daszkiewicz, Dziembowski & Pamyatnykh (2003) can be successfully applied to the extremely interesting pulsating subdwarf Bal09.

2 BALLOON 090100001

Bal09 is presently the brightest known sdBV star. Its pulsations were found by Oreiro et al. (2004) from a single night of photometric data. The main mode detected in this star has a semi-

* E-mail: andy@astro.as.ap.krakow.pl

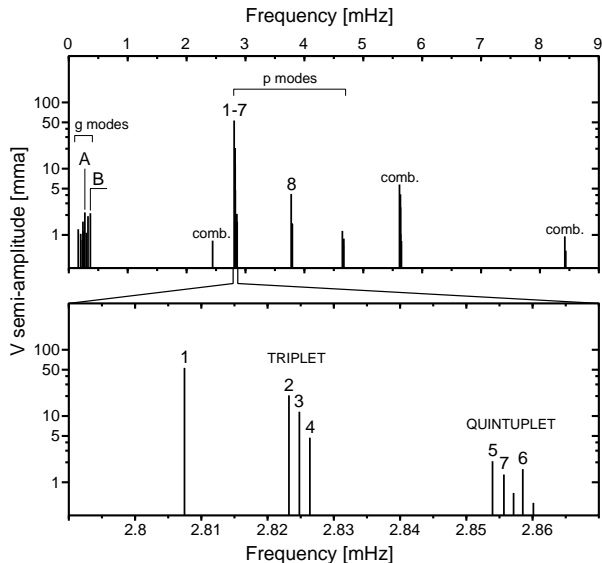


Figure 1. A schematic Fourier spectrum of the 2004 *B*-filter data of Bal 09. Note that semi-amplitudes are given on a logarithmic scale. Modes with the largest amplitudes are labelled as in Paper I and Tables 1 and 2. Two components of the quintuplet (not labelled in the bottom panel) were detected only in the Fourier spectrum of 2005 data.

amplitude of about 60 mmag in *B* and a period of about 6 min, quite long for a V361 Hya star. Thus, Bal 09 became an obvious target for a more detailed study. The follow-up photometry carried out in 2004 (Baran et al. 2005, hereafter Paper I; Oreiro et al. 2005) revealed several interesting features in its frequency spectrum (Fig. 1). First of all, among about 20 detected modes, an equidistant triplet was found close to the main mode. If interpreted in terms of rotational splitting, it would imply a rotational period of about 7 d (Paper I). Even more importantly, several low-frequency *g* modes were found. This made the star one of two presently known hybrid V361 Hya/PG 1716 stars; the other one is HS 0702+6043 (Schuh et al. 2006).

In 2005, a large multisite campaign was carried out on Bal 09 (Baran et al., in preparation). The new data allowed the detection of a quintuplet (see Fig. 1) whose three strongest components had already been detected in the 2004 data. In addition, it turned out that the amplitudes of some modes change. However, the most surprising discovery was finding that splittings of multiplets changed considerably between 2004 and 2005 (Baran et al. 2007). As far as we are aware, this is the first clear evidence for such a change in any pulsating star. This finding poses a problem for the interpretation of splittings only in terms of rotation. However, we believe that rotation is the main factor that causes splittings, while another (presently unknown) effect(s) causes its small variations. We therefore refer to the multiplets as rotationally split.

3 OBSERVATIONS AND ANALYSIS

The amplitude changes detected in Bal 09 and other sdBV stars suggest that if one wants to combine photometry and spectroscopy for mode identification, the data must be obtained simultaneously. For this reason, we decided to use the multiband photometry of Paper I and spectroscopy of TO06 which were coincidentally acquired at the same time, during 2004 August and September.

The *UBVR* photometry of Paper I was carried out at two sites, Mt. Suhora and Loiano Observatories. About 120 h of data were gathered through each filter. The observations were spread over about 40 d, resulting in a frequency resolution of better than $0.5 \mu\text{Hz}$. Details of the Fourier analysis of these data can be found in the Paper I. As found in that paper, the frequency spectrum of Bal 09 shows three regions of *p* modes (around 2.8, 3.8 and 4.7 mHz), a group of low-frequency (below 0.5 mHz) *g* modes and three regions where combination modes occur, labeled ‘comb.’ in Fig. 1.

Because the changes in amplitude appeared to be more pronounced in the 2005 campaign data than we found in Paper I, we decided to reanalyze the 2004 photometry. This time, however, we allowed for linear amplitude changes. In addition, the outliers were removed with a slightly more stringent criterion than in Paper I. This resulted in a lower detection threshold. We also decided to accept only those modes which were detected in all four filters. As a consequence, the list of modes we present in Tab. 3 is shorter than in Paper I.

As mentioned above, spectroscopic observations of Bal 09 were carried out by TO06, simultaneously with the 2004 photometry. During seven nights spanning over 38 d, they obtained over 2500 low-resolution spectra. Importantly the cycle time was only 43 s long, allowing good sampling of the radial velocity curve. Details of the reduction and analysis can be found in TO06. We have reanalyzed the radial-velocity data of TO06 in order to obtain the fit parameters in a manner consistent with the photometry. As the 2004 photometric data suffered from aliasing much less than the radial-velocity data of TO06, we always adopted a frequency measured from photometry, even if the alias peak was found to be higher than that at the “real” frequency. In total, we detected 14 modes in radial velocity; their parameters are presented in Tab. 1. We found the same *p* modes as TO06: f_1 , the triplet (f_2 , f_3 , and f_4), f_8 and two combination frequencies, $2f_1$ and $f_1 + f_2$. In the low-frequency domain, we also detected seven modes above the detection level. Unfortunately, none of these could be unambiguously identified with the modes detected in photometry, and only some of these were the same as those reported by TO06. Apparently, the rich spectrum of *g* modes and their very low amplitudes make the aliasing a very severe problem during the prewhitening procedure.

However, three *g* modes known from photometry, f_A , f_B and f_C according to the designations used in Tab. 3, were found by TO06 in the variations of the equivalent widths (EW) of the Balmer H γ –H9 lines. The reason why the same modes were not detected in radial velocities can be qualitatively explained if we recall that for *g* modes the horizontal motions dominate the radial motions, while for *p* modes the opposite is true. As all have small amplitudes, it is therefore quite possible that different modes are seen in photometry (and EW changes) and radial velocities. As shown by For et al. (2006), because of the small amplitudes of *g* modes, it is very difficult to detect them in radial-velocity data. For modes observed in both photometry and spectroscopy, simultaneous data allow us to derive phase lags between light and radial-velocity variations. This parameter is related to the non-adiabacity of pulsations. The phase lags for modes detected in photometry and spectroscopy are given in Tab. 1. The weighted mean of the phase lag for five independent *p* modes is equal to 1.45 ± 0.03 rad or $83 \pm 2^\circ$. For the dominant mode, f_1 , it is very similar, 1.43 ± 0.02 rad. Because this mode is radial (see Sect. 5), the phase of maximum brightness corresponds roughly to the phase of minimum radius. In other words, we can conclude that in V361 Hya stars the brightness variations are dominated by the temperature effects. Adopting projection factor equal

Table 1. The results of re-analysis of 2004 *UBVR* data of Bal09. Semi-amplitudes, A , and phases, ϕ , are given for the epoch HJD = 2 453 250.

Mode	Mean frequency [mHz]	A [mma]				ϕ [rad]				dA/dt [mma/d]			
		U	B	V	R	U	B	V	R	U	B	V	R
f_A	0.272362(6)	2.72(20)	2.43(14)	2.04(14)	2.19(14)	0.27(08)	0.25(07)	0.23(08)	0.17(07)	-0.031(19)	-0.046(13)	-0.035(10)	-0.038(13)
f_B	0.365805(5)	3.23(20)	2.59(14)	2.25(14)	2.10(14)	4.56(06)	4.72(06)	4.59(06)	4.57(07)	+0.007(19)	-0.018(13)	-0.008(10)	-0.019(13)
f_C	0.325653(8)	2.07(20)	1.50(14)	1.58(14)	1.33(14)	4.96(10)	4.92(10)	5.00(08)	4.71(11)	+0.021(19)	+0.048(13)	+0.034(10)	+0.040(13)
f_D	0.239957(5)	2.25(20)	2.07(14)	1.68(14)	1.77(14)	5.25(09)	5.20(07)	5.15(08)	5.17(08)	+0.061(19)	+0.007(13)	-0.003(10)	+0.043(13)
f_1	2.8074698(2)	69.03(22)	53.00(15)	48.53(16)	46.34(15)	4.30(01)	4.32(01)	4.31(01)	4.31(01)	+0.085(21)	+0.065(15)	+0.081(11)	+0.065(14)
f_2	2.8232355(7)	25.13(23)	20.49(16)	18.75(16)	18.38(15)	5.06(01)	5.07(01)	5.08(01)	5.06(01)	+0.059(22)	+0.001(15)	+0.048(13)	+0.006(15)
f_3	2.824809(1)	14.43(23)	11.83(17)	11.00(15)	10.93(16)	1.31(02)	1.28(01)	1.30(01)	1.30(01)	-0.070(23)	-0.033(17)	-0.029(13)	-0.060(16)
f_4	2.826387(3)	5.12(23)	4.79(16)	4.27(16)	4.03(16)	1.44(05)	1.41(03)	1.36(04)	1.42(04)	-0.024(21)	+0.007(15)	-0.002(13)	+0.019(15)
f_5	2.853963(10)	1.88(23)	1.57(16)	1.63(17)	1.26(16)	0.98(12)	0.63(10)	0.81(09)	0.99(12)	-0.001(25)	+0.018(18)	+0.017(13)	+0.006(17)
f_6	2.858536(12)	1.88(23)	1.39(17)	1.50(17)	0.98(17)	4.09(12)	4.10(14)	4.18(13)	4.11(19)	+0.023(24)	-0.024(17)	-0.018(13)	-0.017(15)
f_7	2.855698(11)	1.91(24)	1.75(18)	1.39(16)	1.08(16)	2.20(13)	1.78(10)	2.00(17)	1.92(15)	-0.007(21)	-0.016(15)	-0.039(12)	-0.006(15)
f_8	3.776106(3)	5.66(21)	4.37(15)	3.90(14)	3.72(14)	0.96(04)	0.96(04)	0.89(04)	0.93(04)	+0.012(21)	-0.030(14)	+0.004(11)	-0.008(14)
f_9	3.786796(9)	2.28(22)	1.81(16)	1.72(15)	1.56(15)	0.54(10)	0.35(10)	0.41(09)	0.41(11)	-0.025(21)	-0.018(15)	-0.013(11)	-0.034(14)
f_{10}	3.795581(14)	1.12(22)	0.99(16)	1.03(15)	0.82(15)	5.94(19)	0.10(16)	5.61(13)	6.04(20)	+0.001(21)	+0.010(15)	+0.026(11)	+0.039(14)
f_{14}	3.809277(17)	1.01(21)	1.15(15)	0.64(14)	0.92(14)	6.01(21)	5.73(13)	5.45(38)	5.88(19)	+0.027(21)	+0.009(15)	-0.022(11)	-0.030(14)
f_{11}	4.645122(8)	1.20(20)	1.15(14)	1.01(14)	0.99(14)	1.10(17)	1.28(13)	0.84(13)	1.41(15)	-0.002(19)	-0.012(14)	+0.004(10)	-0.020(13)
f_{12}	4.669244(15)	0.96(20)	1.38(14)	0.87(14)	0.77(14)	5.26(22)	5.25(12)	5.25(24)	5.86(18)	-0.011(19)	-0.025(14)	-0.025(10)	+0.015(13)
f_1-f_B	2.4416648	0.72(20)	0.75(14)	0.61(14)	0.50(14)	6.28(20)	0.12(18)	6.11(17)	0.11(25)	+0.053(19)	+0.015(13)	+0.009(10)	+0.011(13)
$2f_1$	5.6149396	6.78(21)	5.48(15)	5.18(15)	4.75(14)	0.78(03)	0.83(03)	0.90(02)	0.85(03)	-0.036(20)	+0.014(14)	+0.020(11)	-0.005(13)
f_1+f_2	5.6307053	5.05(22)	4.21(16)	3.83(16)	3.68(15)	1.63(04)	1.63(04)	1.69(04)	1.65(04)	+0.019(21)	-0.001(15)	-0.010(12)	+0.019(14)
f_1+f_3	5.6322788	2.51(23)	2.35(16)	2.20(15)	2.20(15)	4.28(07)	4.31(07)	4.24(06)	4.29(06)	+0.026(22)	-0.013(15)	-0.016(12)	+0.005(15)
f_1+f_4	5.6338568	0.80(22)	0.83(16)	0.91(15)	0.74(15)	3.70(27)	4.43(19)	3.96(15)	3.85(19)	-0.029(21)	-0.009(14)	-0.009(11)	+0.002(14)
$3f_1$	8.4224094	1.02(20)	0.61(15)	0.73(15)	0.91(14)	4.04(21)	3.79(24)	4.12(13)	4.04(15)	-0.005(19)	-0.019(14)	+0.023(11)	+0.001(13)
$2f_1+f_2$	8.4381751	0.41(20)	0.27(15)	0.45(15)	0.91(14)	4.00(20)	3.83(32)	5.04(20)	4.47(13)	+0.021(19)	+0.028(14)	+0.018(11)	+0.029(13)

Table 1. Results of the sine-curve fit to the low-resolution spectroscopic data of TO06. As for the photometric data (Tab. 3), the phases are given for the epoch HJD = 2 453 250. $\Delta\phi = \phi_{\text{RV}} - \phi_{\text{phot}}$ denotes difference between radial-velocity and photometric (averaged over all four filters) phases.

Mode	Frequency [mHz]	Semi-amplitude [km s ⁻¹]	ϕ_{RV} [rad]	$\Delta\phi$ [rad]
f_1	2.8074698	19.16(20)	5.74(01)	+1.43(02)
f_2	2.8232355	5.97(25)	0.33(04)	+1.54(04)
f_3	2.824809	3.64(26)	2.66(07)	+1.36(07)
f_4	2.826387	1.39(24)	3.12(18)	+1.71(18)
f_8	3.776106	1.11(18)	2.38(17)	+1.45(17)
$2f_1$	5.6149396	1.23(19)	1.98(15)	+1.14(15)
f_1+f_2	5.6307053	1.10(19)	3.28(17)	+1.63(17)
TO06	0.32812(3)	2.12(19)	5.37(09)	—
TO06 alias	0.36614(4)	1.15(19)	3.27(17)	—
	0.16944(3)	1.36(19)	0.63(14)	—
TO06	0.46406(3)	1.16(19)	4.46(16)	—
	0.29727(4)	1.51(20)	3.64(13)	—
	0.26247(4)	1.21(19)	1.81(16)	—

to 1.4 as typical for an sdB star (see Montañés Rodríguez & Jeffery 2001) and a radius of $0.25 R_{\odot}$, we estimate the full range of radius variations for the dominant mode in Bal09 to be about 1.7 per cent.

4 THE METHOD OF MODE IDENTIFICATION

Having derived frequencies, amplitudes and phases we can now apply the method (described in detail by Daszyńska-Daszkiewicz et al. (2003)) to discriminate ℓ parameters for the modes detected in our photometry and spectroscopy of Bal09.

In the simplest form, the method of Daszyńska-Daszkiewicz et al. (2003) utilizes a set of linear equations, of the form

$$\mathcal{D}_{\lambda,\ell}(\tilde{\varepsilon}f) + \mathcal{E}_{\lambda,\ell}\tilde{\varepsilon} = A_{\lambda} \quad (1)$$

to derive two complex parameters, $\tilde{\varepsilon}$ and f . The coefficients A_{λ} are taken from observations; these are amplitudes, a_{λ} , and phases, ϕ_{λ} , written in a complex form, $A_{\lambda} = a_{\lambda} \exp(i\phi_{\lambda})$, where λ denotes a given photometric band. However, $\mathcal{D}_{\lambda,\ell}$ and $\mathcal{E}_{\lambda,\ell}$ depend on the flux and limb darkening derivatives over effective temperature and surface gravity, and have to be calculated using model stellar atmospheres. In principle, observations in two photometric bands are sufficient to solve the set of equation (1) once the spherical degree ℓ is assumed. However, if observations in more than two photometric bands are available, the set becomes overconditioned and can be solved by means of the least-squares method. Usually, however, we are not interested in the values of $\tilde{\varepsilon}$ and f , but in discriminating ℓ . In order to achieve this, the equations are solved for different values of ℓ and then a goodness-of-fit statistic like reduced χ^2 is used to decide on discrimination.

Unfortunately, as was shown by Daszyńska-Daszkiewicz, Dziembowski & Pamyatnykh (2005, see also Sect. 5), using merely photometric data rarely leads to unambiguous discrimination of ℓ . It is much better to combine photometric and spectroscopic data adding another equation of set, that is

$$\mathcal{F}_{\lambda,\ell}\tilde{\varepsilon} = \mathcal{M}_{1,\lambda} \quad (2)$$

In Equation (2), $\mathcal{M}_{1,\lambda}$ represents the first moment of spectral line variations, (i.e. radial velocities), while $\mathcal{F}_{\lambda,\ell}$ is again calculated from the model atmospheres. The solution of a set of equations (1) and (2) leads in this case to a much better discrimination of ℓ (see Section 5).

The model-dependent coefficients in equations (1) & (2) and, consequently, the discrimination of ℓ depend on the model parameters, in particular effective temperature, surface gravity and metallicity. For Bal09, the effective temperature and surface gravity were derived by Oreiro et al. (2004), $T_{\text{eff}} = 29\,450 \pm 500$ K, $\log g = 5.33 \pm 0.10$ dex and Telting et al. (2006), $T_{\text{eff}} = 28\,700$ K, $\log g = 5.39$ dex. We therefore calculated flux distributions in the range between 300 and 1000 nm for a grid of models with T_{eff} ranging from 28 100 and 31 000 K and $\log g$ from 5.2 to 5.5 dex. To do this, a grid of fully metal line-blanketed local thermodynamic equilibrium (LTE) stellar atmosphere models was calculated with the ATLAS9 code of Kurucz (1992). Flux distributions were then calculated using Michael Lemke’s version of the LINFOR program (originally developed by Holweger, Steffen, and Steenbock at Kiel University), similar to the synthetic spectra used by O’Toole & Heber (2006). The Kurucz line list was used as a source of oscillator strengths and damping constants for all metal lines. Only lines that have been observed experimentally were included. The resulting flux distributions were multiplied by transmission functions of the filters in order to obtain integrated fluxes in the four photometric bands, *UBVR*, that we used.

For the same grid of models, we also calculated the specific intensities as a function of $\mu = \cos \theta$, where θ was the angle between the line of sight and the normal to the stellar surface in a given point of the stellar disc. Using these intensities, the limb darkening law was derived, fitting the coefficients c and d of a function

$$I(\mu) = I(1)[1 - c(1 - \mu) - d(1 - \sqrt{\mu})] \quad (3)$$

(Díaz-Cordovés & Giménez 1992) which was found to reproduce best the calculated changes of $I(\mu)$. This was carried out for different combinations of input parameters of the model, thus allowing the calculation of necessary derivatives.

The flux distribution calculated from a model atmosphere depends also on helium abundance, metallicity and microturbulent velocity. Following the determination of Oreiro et al. (2004), helium abundance was assumed to be $\log[n(\text{He})/n(\text{H})] = -2.54$. In addition, we assumed solar metallicity and microturbulent velocity $\xi = 0$ km s⁻¹. The latter two parameters have not been determined yet for Bal09, but are typical values for an sdB star (e.g. O’Toole & Heber 2006).

5 DISCRIMINATION OF THE ℓ PARAMETER

As a first step, we used the method presented in Section 4 in its simplest form (i.e. taking into account only photometric amplitudes and phases in four bands; see Tab. 3). The results for six modes detected both in photometry and radial velocities are presented in Tab. 2 and in the left panels of Fig. 2. We limited our calculations to $\ell \leq 4$ because, as a result of averaging over the stellar disc, modes with larger ℓ are not expected to be visible in photometry.

As can be seen from Fig. 2 and Tab. 2, there is only little discrimination of ℓ for f_1 , f_2 and f_3 and none for f_4 and f_5 . For f_1 , $\ell = 0$ or 2 are possible, while for f_2 and f_3 , $\ell > 2$ are excluded.

The poor discrimination of ℓ when using photometric data can be understood when considering the amplitude ratios versus wavelength calculations carried out by Ramachandran et al. (2004). In

Table 2. The results of the application of the method of Daszyńska-Daszkiewicz et al. (2003) for Bal09 2004 photometric data: reduced χ^2 values for five modes with the largest amplitudes as a function of the spherical degree ℓ .

ℓ	f_1	f_2	f_3	f_4	f_8
0	3.56	1.10	0.81	0.48	0.26
1	13.22	1.03	0.89	0.84	0.28
2	7.48	1.09	0.89	0.57	0.18
3	42.12	10.67	5.21	0.46	0.43
4	28.39	5.07	2.30	0.34	0.46

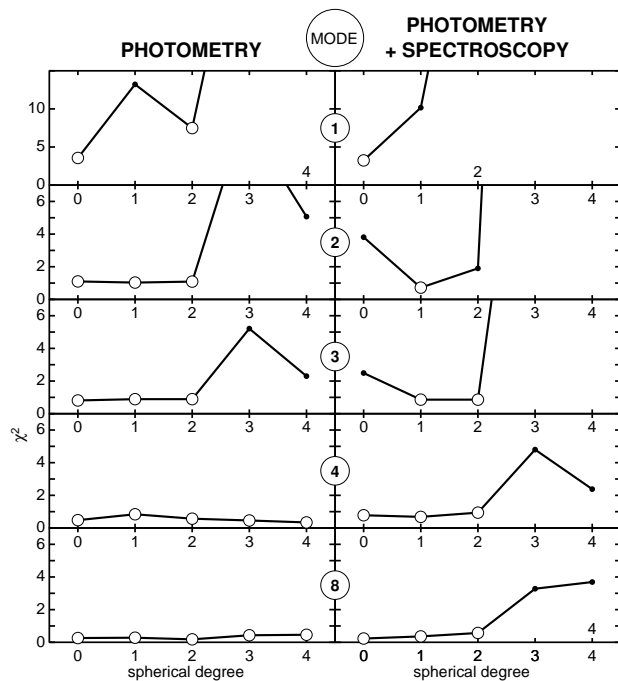


Figure 2. Reduced χ^2 as a function of the spherical degree ℓ for 2004 data of Bal09 and five modes detected both in photometry and spectroscopy. The modes are labelled with the encircled designation in the middle (see Tables 3 and 1). Left panels show the results when only photometric data were used in calculations, and right panels when photometric and spectroscopic data were combined. The ℓ value(s) that we regard as possible for a given mode are shown with large circles.

addition, three of the four photometric bands we used are located in the Paschen continuum. The resulting equations for different bands might therefore be highly correlated, which will not lead to a good discrimination of ℓ .

It also has to be pointed out that the reduced χ^2 statistics we use to discriminate ℓ , does not have, in our case, its proper characteristics, as the set of equation (1) is not well overconditioned; it has only four degrees of freedom. For this reason, we did not set a given threshold in χ^2 to indicate possible values of ℓ . Instead, we do this arbitrarily, comparing the values of χ^2 for different values of ℓ ; those with the smallest χ^2 are regarded as possible (see Fig. 2).

In the next step, we added the radial velocity data as an additional constraint via equation (2) and repeated the procedure. The results are shown in the right panels of Fig. 2 and in Tab. 3. As equation (2) contains only $\tilde{\varepsilon}$ as a free parameter, it is expected that f and $\tilde{\varepsilon}$ will be much better constrained than previously and, con-

Table 3. The same as in Tab. 2, but for the combined photometric and spectroscopic data.

ℓ	f_1	f_2	f_3	f_4	f_8
0	3.88	4.44	3.03	0.96	0.22
1	9.03	0.80	0.94	0.65	0.35
2	47.73	1.99	1.06	0.51	0.55
3	218.07	77.42	28.11	4.63	3.56
4	1526.90	101.09	35.45	6.03	6.03

Table 4. The possible values of ℓ for five strongest modes in Bal09 derived in this paper and by Tremblay et al. (2006).

Mode	This paper (photometry)	This paper (photometry + spectroscopy)	Tremblay et al. (2006)
f_1	0, 2	0	0, 1
f_2	0, 1, 2	1	1, 2
f_3	0, 1, 2	1, 2	1, 2
f_4	0, 1, 2, 3, 4	0, 1, 2	1, 2, 4
f_8	0, 1, 2, 3, 4	0, 1, 2	0, 1, 2, 3

sequently, ℓ will be much better discriminated. As can be seen from Fig. 2, this is indeed the case. Adding spectroscopy improves the situation in the sense that observational equations become less correlated, which allows reliable estimation of ε and f , but not as far as the χ^2 statistics is concerned. For combined data, the problem has two more (i.e. six) degrees of freedom, still too small a number to say the problem is well defined. Because of that, we would like to avoid giving a level of significance, as it would be irrelevant. Nevertheless, relative numbers tell us which values of ℓ are acceptable, although, as we have pointed out, our choice is arbitrary.

The best and least ambiguous discrimination was obtained for the dominant mode, which appears to be radial ($\ell = 0$). For the strongest component of the triplet, f_2 , $\ell = 1$ is definitely the best solution, exactly as expected. For the two remaining triplet components, f_3 and f_4 , ℓ is not unambiguously identified, but $\ell = 1$ is one of the possibilities. Therefore, we conclude that, as already suggested in Paper I, the main mode in Bal09 is radial, while the triplet represents a rotationally split $\ell = 1$ mode.

Table 4 summarizes the results of our discrimination. In addition, we compare these results with those presented by Tremblay et al. (2006), who used only photometric data to identify ℓ for the nine modes published in Paper I. They did not obtain a unique identification for any of these modes. For the best cases, they present two possible values of ℓ , similar to the results we obtained using only the photometric data.

We also checked how the discrimination we obtain depends on the parameters of the model. The result for adopting five different effective temperatures from the range between 28 500 and 30 500 K is shown in Fig. 3. The change with T_{eff} does not greatly affect the result of discrimination, although lower effective temperatures $\ell = 1$ for f_1 and $\ell = 2$ for f_2 become alternatives to those given in Tab. 4. A negligible effect was obtained while changing the mass between 0.47 and 0.53 M_{\odot} and radius between 0.23 and 0.26 R_{\odot} .

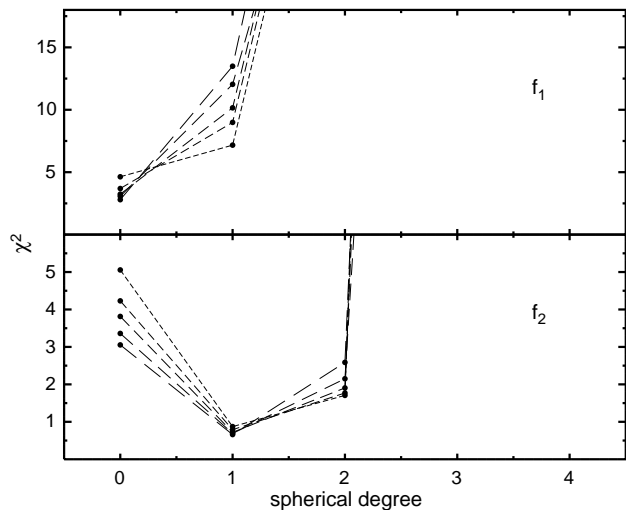


Figure 3. Discrimination of the ℓ parameter for five different values of T_{eff} , combined photometry and spectroscopy and two strongest modes, f_1 (top) and f_2 (bottom). Going from the shortest to the longest dashes results are shown for effective temperatures between 28 500 and 30 500 K in 500-K steps.

6 SUMMARY AND CONCLUSIONS

Using photometric and spectroscopic data for Bal09, we have shown that the method of mode identification developed by Daszyńska-Daszkiewicz et al. (2003) can be successfully applied to Bal09. We believe that, if simultaneous multicolour photometry and spectroscopy are carried out, the method will also allow mode identification in other sdBV stars. In Bal09, the spherical degree ℓ was unambiguously identified for the two modes with the largest amplitudes. For several other modes, we limited the number of possible values of ℓ to two or three. If we accept that the two observed multiplets are caused by rotational splitting, then the number of identified modes increases to nine: the triplet components have $\ell = 1$, the quintuplet components, $\ell = 2$.

It is clear from our considerations that photometry itself is not sufficient to identify mode satisfactorily for sdBV stars, and that adding spectroscopic observations greatly improves the situation. For Bal09, it is certainly worth carrying out another photometric and spectroscopic campaign to identify modes with even lower amplitudes. However, our identification is probably sufficient to go a step further and attempt asteroseismology of this star. However, for this purpose, an appropriate set of models is required. A first attempt was presented in Paper I using the models of Charpinet et al. (2002). While we had no modes identified at that time, the assumption that the main mode is radial now appears to be correct. With reliable identification of modes from the 2.8 mHz group, a good seismic model that fits the identified modes might be used to match (and identify) remaining modes. In order to carry out a thorough asteroseismological analysis and potentially learn new physics, it is important that more modes are identified independent of pulsation models in sdBV stars. We have provided a crucial piece of the puzzle, and the challenge is now for pulsation theorists to find models that match both the pulsation frequencies and mode identifications derived here.

ACKNOWLEDGMENTS

This project was partially supported by grant no. 1P03D 013 29 kindly provided by Polish MNiSW. Constructive criticism from the anonymous referee is also acknowledged.

REFERENCES

- Baran A., Pigulski A., Koziel D., et al., 2005, *MNRAS*, 360, 737 (Paper I)
- Baran A., Oreiro R., Pigulski A., et al., 2007, *Proc. of the 15th European White Dwarf Workshop EUROWD06*, 372, 607
- Charpinet S., Fontaine G., Brassard P., Dorman B., 2002, *ApJS*, 140, 469
- Daszyńska-Daszkiewicz J., Dziembowski W.A., Pamyatnykh A.A., 2003, *A&A*, 407, 999
- Daszyńska-Daszkiewicz J., Dziembowski W.A., Pamyatnykh A.A., 2005, *A&A*, 441, 641
- Díaz-Cordovés, J., & Giménez, A., 1992, *A&A*, 259, 227
- Falter S., Heber U., Dreizler S., et al., 2003, *A&A*, 401, 289
- For B.-Q., Green E.M., O’Donoghue D., et al., 2006, *ApJ*, 642, 1117
- Jeffery C.S., Pollacco D., 2000, *MNRAS*, 318, 974
- Jeffery C.S., Dhillon V.S., Marsh T.R., Ramachandran B., 2004, *MNRAS*, 352, 699
- Jeffery C.S., Aerts C., Dhillon V.S., Marsh T.R., Gänsicke B., 2005, *MNRAS*, 318, 974
- Kilkenny D., Koen C., O’Donoghue D., et al., 1997, *MNRAS*, 285, 640
- Koen C., 1998, *MNRAS*, 300, 567
- Kurucz R.L., 1992, in: *The Stellar Populations of Galaxies*, IAU Coll. 149, eds. B.Barbuy & A. Renzini, Kluwer Academic Publishers, Dordrecht, p. 225.
- Montañés Rodríguez P., Jeffery C.S., 2001, *A&A*, 375, 411
- Oreiro R., Ulla A., Pérez Hernández F., et al., 2004, *A&A*, 418, 243
- Oreiro R., Pérez Hernández F., Ulla A., et al., 2005, *A&A*, 438, 257
- O’Toole S.J., Heber U., 2006, *A&A*, 452, 579
- O’Toole S.J., Bedding T.R., Kjeldsen H., et al., 2000, *ApJ*, 537, L53
- O’Toole S.J., Bedding T.R., Kjeldsen H., Dall T.H., Stello D., 2002, *MNRAS*, 334, 471
- O’Toole S.J., Jørgensen M.S., Kjeldsen H., Bedding T.R., Dall T.H., Heber U., 2003, *MNRAS*, 340, 856
- O’Toole S.J., Heber U., Jeffery C.S., et al., 2005, *A&A*, 440, 667
- Ramachandran B., Jeffery C.S., Townsend R.H.D., 2005, *A&A*, 428, 209
- Schuh S., Huber J., Dreizler S., et al., 2006, *A&A*, 445, 31
- Telting J.H., Østensen R.H., 2006, *A&A*, 450, 1149 (TO06)
- Telting J.H., Østensen R.H., Heber U., Augusteijn T., 2006, *Baltic Astron.*, 15, 235
- Tremblay P.E., Fontaine G., Brassard P., Bergeron P., Randall S.K., 2006, *ApJS*, 165, 551
- Wolf V.M., Jeffery C.S., Pollacco D.L., 2002, *MNRAS*, 329, 497